

Surface Chemistry of “Unprotected” Nanoparticles: A Spectroscopic Investigation on Colloidal Particles

Imke Schrader,[†] Jonas Warneke,[†] Sarah Neumann,[†] Sarah Grotheer,[†] Andreas Abildgaard Swane,[‡] Jacob J. K. Kirkensgaard,[§] Matthias Arenz,[‡] and Sebastian Kunz^{*,†}

[†]Institute for Applied and Physical Chemistry (IAPC), Faculty 2, University of Bremen, Leobenerstraße, 28359 Bremen, Germany

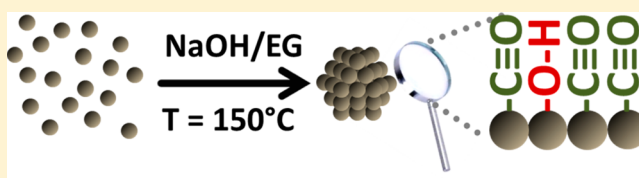
[‡]Nano-Science Center, Department of Chemistry, University of Copenhagen, Universitetsparken 5, DK-2100 Copenhagen Ø, Denmark

[§]Niels Bohr Institute, University of Copenhagen, Universitetsparken 5, DK-2100 Copenhagen Ø, Denmark

S Supporting Information

ABSTRACT: The preparation of colloidal nanoparticles in alkaline ethylene glycol is a powerful approach for the preparation of model catalysts and ligand-functionalized nanoparticles. For these systems the term “unprotected” nanoparticles has been established because no strongly binding stabilizers are required to achieve stable colloids. Irrespective of this fact, the particles must be considered as being covered

by adsorbates, as otherwise the particles would coalesce and precipitate. The identification of these protecting adsorbate species is however still under debate and is the scope of the present study. “Unprotected” Pt and Ru nanoparticles were characterized by NMR spectroscopy, which does not evidence the presence of any C–H containing species bound to the particle surface. Instead, the colloids were found to be covered by CO, as demonstrated by IR spectroscopy. However, analysis of the stretching mode reveals the presence of a second species. On the basis of the spectroscopic characterization this species is concluded to be OH[−], and it is demonstrated that the applied synthesis route results only in stable colloids if OH[−] is present within the reaction mixture. IR spectroscopy reveals that the CO coverage increases as the NaOH concentration used in the precursor solution is decreased. However, even at the lowest for the synthesis suitable OH[−] concentration the surface was found to be covered by both species. Finally, the effect of the OH[−] concentration on the particle size distribution was studied. The maximum was found to shift to larger particle diameters as the OH[−] concentration is lowered which is accompanied by broadening of the size distribution.



1. INTRODUCTION

Colloidal synthesis methods are a versatile approach for the preparation of nanoparticles and enable the control of properties such as the size, shape, and for bimetallic materials the chemical composition.^{1–4} Due to their high surface to bulk ratio such nanostructures are from a thermodynamic perspective not stable and tend to minimize their free surface energy by sintering. The typical strategy to achieve stable colloidal nanoparticles is the use of stabilizers that bind to their surface, which leads to a reduction of the free surface energy and shields the particle surface sterically. For catalytic applications these stabilizers have to be removed because they block the surface and thus reaction sites. This can often be a challenging task when strongly binding groups are involved (e.g., thiols) or if carbonaceous species are formed during stabilizer removal.⁵ These limitations exclude the use of various established colloidal syntheses for model studies in catalysis and requests for the development of protocols that avoid the use of any strongly binding stabilizers.⁶

The above-discussed limitations of colloidal methods for the preparation of model catalysts can be overcome by a synthesis strategy named the “polyol approach”. The term covers the

synthesis of particles in alkaline ethylene glycol (EG).⁷ For Pt, Ru, and Rh this approach allows for the preparation of particles in the nanometer regime, without the need for any strongly stabilizing species (amines, phosphines, or thiols).⁸ Therefore, the term “unprotected” was established for nanoparticles prepared by this approach.^{8–10}

The use of these “unprotected” particles allows for the preparation of model catalysts without the need for any high-temperature post treatment that might corrupt the particle size distribution by sintering.^{11,12} As a result, aspects such as support or coverage effects can be studied in a systematic manner.^{13,14} Another emerging research field for which “unprotected” particles are extremely beneficial is the functionalization of nanoparticles. It has been demonstrated that organic molecules (ligands) can be bound to “unprotected” particles in a separate step, while the particle size is maintained.^{10,15,16} This enables investigation of the influence

Received: April 22, 2015

Revised: July 13, 2015

of the ligand on the particle properties in a systematic manner because the particle and ligand can be varied independently.

From a physicochemical perspective the term “unprotected” is clearly misleading. Surface science teaches that clean or adsorbate-free surfaces can only be generated under UHV (ultrahigh vacuum) conditions.¹⁷ These conditions are clearly not met by the preparation conditions applied for “unprotected” nanoparticles. Despite the fact the original synthesis recipe is already 15 years old and used by several groups, the question how “unprotected” nanoparticles are actually protected is still under debate. Certainly it would be beneficial to understand the surface chemistry of the materials for further developing the alkaline polyol synthesis. So far, the published work on “unprotected” nanoparticles usually covers mainly preparative chemical strategies or the analysis of the organic compounds within the reaction medium.^{8,18,19} Such experiments do however not allow for probing what is actually bound to the surface of the particles. The presented work hence focuses on the characterization of “unprotected” nanoparticles by means of spectroscopic methods (NMR and IR) in order to determine what actually protects “unprotected” nanoparticles. While in most previous investigations the importance of specific organic species was discussed, we found spectroscopically no evidence for the presence of surface-bound C–H containing species. Instead, IR spectroscopy reveals that “unprotected” nanoparticles are covered by CO that is diluted by another adsorbate and proposed to be OH[−]. It is shown that the presence of OH[−] for the synthesis is essential in order to obtain stable colloids and one key to manipulate the preparation process.

2. EXPERIMENTAL SECTION

2.1. Material Synthesis. **2.1.1. Synthesis of “Unprotected” Pt Nanoparticles.** For the preparation of “unprotected” Pt nanoparticles via the standard route applied by us, 0.25 g of H₂PtCl₆·H₂O (40 wt % metal, ChemPur) was dissolved in 25 mL of ethylene glycol (EG) (99.8%, Sigma-Aldrich) in a 250 mL glass flask. A solution of 0.50 g of NaOH (98.9%, Fisher Chemical) dissolved in 25 mL of EG was added and the mixture vigorously stirred at 500 rpm (stir bar length = 2.5 cm) to ensure proper mixing of the two solutions. For the preparation of “unprotected” particles with different OH[−] concentrations, the NaOH concentration of the EG solution was adjusted accordingly prior to mixing with the Pt precursor solution. The term “starting OH[−] concentration” that is used in the following refers to the NaOH concentration after mixing metal precursor and alkaline EG solutions. The flask was equipped with a reflux condenser, and the precursor solution was heated to 150 °C using a preheated oil bath. The stirring rate was maintained at 500 rpm. The yellow solution turned black after about 5 min indicating the formation of Pt nanoparticles. The reaction mixture was kept at 150 °C for 1.5 h to ensure complete reduction of the Pt precursor followed by cooling to ambient temperature.

2.1.2. Synthesis of “Unprotected” Ru Nanoparticles. “Unprotected” Ru nanoparticles were prepared by exactly the same procedure as those for the Pt particles (2.1.1), but using RuCl₃·H₂O (40–49 wt % metal, Sigma-Aldrich) as precursor. In order to achieve the same metal concentration as for the Pt nanoparticle synthesis 0.103 g of RuCl₃·H₂O was dissolved in 25 mL of EG prior to mixing with alkaline EG.

2.2. Cleaning of “Unprotected” Nanoparticles. For spectroscopic investigations the as-prepared “unprotected”

nanoparticles have to be cleaned from any nonbinding residues that may overlap with the spectroscopic features of interest and weaken their significance. Therefore, the colloids were precipitated by adding two and eight aliquots of 1 M HCl (VWR) to Pt and Ru particles, respectively. The precipitated colloids were isolated by centrifugation; the supernatant solvent was removed; and the particles were suspended in 1 M HCl. After centrifuging, the supernatant solvent was again removed, and the particles were then redispersed in any desired solvent for the spectroscopic characterization. Application of this procedure enables for cleaning without causing particle sintering as previously shown in various studies.^{8,11,13}

2.3. Mass Spectrometry. Electrospray ionization mass spectrometry (ESI-MS) measurements were performed on a Bruker Esquire-LC ion trap mass spectrometer. In order to analyze all organic species that appear within the reaction mixture, nanoparticles were precipitated by lowering the pH value as described in section 2.2, and the precipitated particles were separated from supernatant solvent by centrifugation. The pH value of the supernatant was subsequently increased into the strong alkaline regime by adding 1 aliquot of 1 M NaOH. The sample was then injected into the mass spectrometer via a syringe pump at a flow rate of 3 μL min^{−1}. Spectra were recorded in the positive ion mode for 1 min and averaged.

2.4. NMR Spectroscopy. For NMR spectroscopic investigations the “unprotected” particles were redispersed in acetone-*d*₆ (euriso-top). Recently, we have investigated the same nanoparticles as in the present study, but functionalized with L-proline, using NMR spectroscopy.²⁰ With regard to these experiments we used a particle concentration of 0.0075 M_{NPs} in the present study because at this concentration pronounced ¹H signals were obtained for L-proline-functionalized Pt nanoparticles, and that even allowed for resolving the coupling patterns. In this way a limited sensitivity due to a too low particle concentration can be excluded. Spectra were recorded on a Bruker AVANCE NB-360.

2.5. IR Spectroscopy. IR spectra were recorded in ATR mode on a Thermo-Nicolet Avatar 370 FT-IR spectrometer with a smart performer ATR unit and a ZnSe crystal plate at a resolution of 4 cm^{−1} and taking 48 scans. In order to record spectra of colloidal nanoparticles the dispersion to be investigated was simply dropped onto the ATR crystal. For all colloidal samples pure EG was used as a reference unless otherwise described. As-prepared samples were studied as received after preparation. Cleaned colloids were prepared by precipitating and rinsing as described in sections 2.1 and 2.2, followed by redispersing in 0.5 aliquots of EG.

2.6. Determination of Particle Size Distributions by Small-Angle X-ray Scattering (SAXS). Small-angle X-ray scattering was performed on a SAXSLab instrument installed at the Niels Bohr Institute of the University of Copenhagen. The instrument is equipped with a 100XL + microfocus sealed X-ray tube from Rigaku producing a photon beam with a wavelength of 1.54 Å. The scattering patterns were recorded with a 2D 300 K Pilatus detector from Dectris. The two-dimensional scattering data were azimuthally averaged, normalized by the incident radiation intensity, the sample exposure time, and the transmission, and corrected for background and detector inhomogeneities using standard reduction software. The background measurement was on a pure EG. The radially averaged intensity *I* is given as a function of the scattering vector $q = 4\pi/\lambda \sin(\theta)$, where λ is the wavelength and 2θ the scattering angle.

The background-corrected scattering data were fitted with a model of polydisperse spheres described by a log-normal distribution. The final intensity expression reads

$$I(q) = C \int P_s^2(q, R) V(R) D(R) dR \quad (1)$$

where C is an overall scaling constant; P_s is the sphere form factor; V is the particle volume; and D is the size distribution. The sphere form factor is given by

$$P_s(q, R) = 4\pi R^3 \frac{\sin qR - qR \cos qR}{(qR)^3} \quad (2)$$

and the log-normal distribution

$$D(R) = \frac{1}{R\sigma\sqrt{2\pi}} \exp\left(\frac{-[\ln(R/R_0)]^2}{2\sigma^2}\right) \quad (3)$$

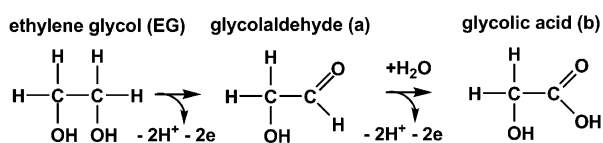
The fits are done using a home written MATLAB code invoking a least-squares X^2 -minimization to optimize correlation between model and data. Thus, the free parameters in the model are the radius and variance of the polydisperse size distribution which are reported below (see Figure 3).

3. RESULTS AND DISCUSSION

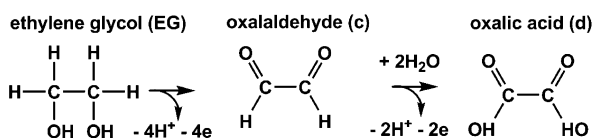
As suitable stabilizers for “unprotected” nanoparticles the following species have been proposed: OH^- , ethylene glycol (EG), glycolate, and acetate (see Scheme 1 for structures and suitable oxidation pathways for EG),¹⁹ the latter two being suitable oxidation products of EG formed during synthesis.^{8,18,19} However, no spectroscopic evidence for the binding of any of these species to “unprotected” nanoparticles has yet been demonstrated. As the reaction medium consists of EG and OH^- , both may account as suitable stabilizers for the

Scheme 1. Oxidation of Ethylene Glycol (EG), Which Is the Reaction That Delivers the Required Electrons for the Reduction of the Metal Precursors, Can Proceed via Three Different Reaction Pathways^a

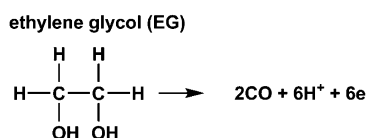
Reaction pathway 1



Reaction pathway 2



Reaction pathway 3



^aEither one of the hydroxyl groups (pathway 1) or both will be oxidized (pathway 2). Alternatively, EG can be directly converted to CO (pathway 3), a reaction that is known to proceed on catalytic metals like Pt.

particles. In order to clarify if glycolate and acetate are possible protecting species their presence within the reaction mixture has to be confirmed, first. Therefore, ESI-MS analysis was performed on the supernatant of the reaction mixture (see Figure S1). The presence of glycolic acid (structure b in Scheme 1) as an oxidation product of EG could be confirmed. Under synthesis conditions the acid will be deprotonated to glycolate because “unprotected” nanoparticles are prepared in an alkaline medium (compare section 2.1). Beside glycolic acid the corresponding aldehyde (structure a in Scheme 1) was found, which is an intermediate formed during oxidation of EG via reaction pathway 1 (Scheme 1). In addition, we identified oxalaldehyde (structure c), which is consistent with a second oxidation reaction pathway for the EG oxidation (see Scheme 1). The concentration of the final product of the second EG oxidation pathway (oxalic acid, structure d in Scheme 1) has previously been determined to be negligible because it readily decomposes to CO_2 and is concluded as being too little to act as a suitable stabilizer for the particles.¹⁹ This conclusion is supported by our results, as no clear evidence for the presence of oxalic acid was found by ESI-MS analysis. None of the discussed and identified EG oxidation pathways (Scheme 1) lead to the formation of acetate. Furthermore, no indication for the formation of acetate was obtained by ESI-MS. It hence seems very unlikely that acetate is stabilizing “unprotected” nanoparticles.

¹H NMR spectroscopy was performed in order to probe if the particles are stabilized by any C–H containing species. A prerequisite for obtaining NMR signals from surface-bound molecules is that either the molecule can rotate on the surface or it exhibits internal rotational degrees of freedom to ensure isotropic relaxation of the nuclear magnetization.²¹ However, even a more rigid structure like L-proline, which is a five-membered ring, hence exhibiting only few internal rotational degrees of freedom, can still be probed by NMR spectroscopy.²⁰ In contrast, all three organic candidates (EG, glycolate, acetate) that have been proposed as stabilizing species and the oxidation intermediates that have been identified via ESI-MS (glycolaldehyde, oxalaldehyde) are quite flexible with internal rotational degrees of freedom. As a result, any of those compounds should be detectable by ¹H NMR spectroscopy, when being bound to the particles. Surface-bound organic molecules can easily be distinguished from the corresponding solvated molecule as the metal core leads to a pronounced downfield of the protons, related to as the Knight shift.^{22,23} Recently, we have investigated L-proline-functionalized Pt nanoparticles prepared from the same “unprotected” Pt colloids discussed here. The NMR spectra revealed a downfield shift of 0.6 ppm for the protons being closest to the surface.²⁰ As a result it should be straightforward to identify and distinguish between the proposed organic compounds being solvated or surface bound.

The NMR spectrum of “unprotected” Pt nanoparticles (Figure 1) reveals the presence of two intensive proton signals at 3.5 and 4.9 ppm (the signal at 2 ppm originates from the solvent, acetone) that can be related to the CH_2 group of EG and OH protons, respectively. The OH protons can be attributed to EG residues that could not be removed completely by sampling rinsing and H_2O that was left within the samples after particle cleaning (see section 2.2). Pure EG was added to test if the signal discussed as CH_2 protons originates from EG bound to the particle surface or merely residues that are dissolved in the solvent. The experiment led to

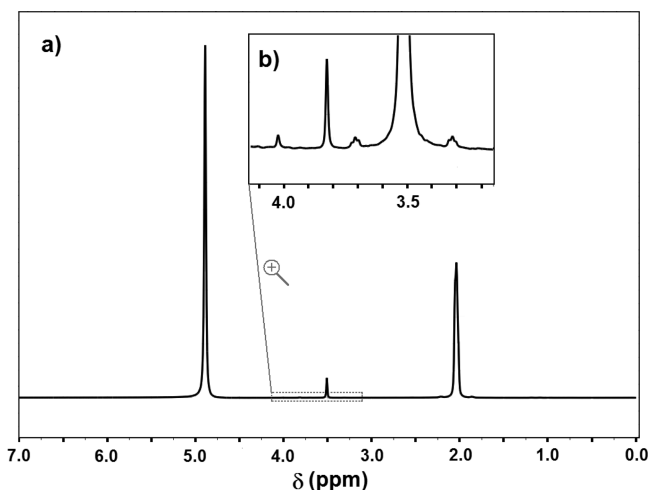


Figure 1. ^1H NMR spectrum (360 MHz, 8.4 T, acetone- d_6) of “unprotected” Pt nanoparticles. The inset (b) shows a zoom in the range from 3.2 to 4.1 ppm.

an increase of the discussed signal (see Figure S2), confirming that the obtained EG is dissolved but not bound to the particle surface. A further detailed analysis of the spectrum shown in Figure 1a by magnifying revealed two additional proton signals at 3.8 and 4 ppm (see inset b in Figure 1; the peaks at 3.3 and 3.7 ppm are ^{13}C satellites of the signal at 3.5 ppm). The signal at 3.8 ppm corresponds to an organic impurity within the deuterated solvent. With respect to the ESI-MS characterization the signal at 4 ppm may correspond to glycolaldehyde, glycolate, or oxalaldehyde (a, b, and c in Scheme 1, respectively). From the chemical shift and the fact that the signal shows no coupling pattern but appears as a singlet, glycolaldehyde and oxalaldehyde can be excluded, and glycolate remains as the sole suitable candidate. Adding pure glycolic acid led to an increase of the signal (see Figure S3). The peak can hence be related to unbound glycolate, which was probably not removed completely by sample rinsing, but not to surface-bound glycolate. Previously, it has been shown that carboxylic ligands cannot be bound to as-prepared “unprotected” Pt nanoparticles because their binding energy on Pt is too low.⁹ This supports our finding that glycolate does not bind to the particles and is hence not suitable to stabilize “unprotected” Pt nanoparticles.

The results obtained for “unprotected” Ru nanoparticles were identical to those of “unprotected” Pt nanoparticles. Two signals at 3.5 and 4.9 ppm that can be related to unbound EG and OH and two small signals at 3.8 and 4 ppm that are assigned to impurities in the deuterated solvent and unbound glycolic acid. A comparison of “unprotected” Pt and Ru nanoparticles can be found in Figure S4. The two metals exhibit different electronic structures and thus cause substantially different Knight shifts.²⁴ As a consequence, the chemical shifts of protons that belong to surface-bound species must be different for the two metal particles. The fact that the chemical shifts are identical hence further supports the conclusion that none of these signals can be attributed to particle-bound species.

In order to explore the presence of any stabilizing species on the particles that cannot be detected by ^1H NMR spectroscopy, “unprotected” Pt particles, cleaned from residual nonbinding species (see section 2.2) were investigated by ATR-IR spectroscopy (black spectrum in Figure 2). The reference

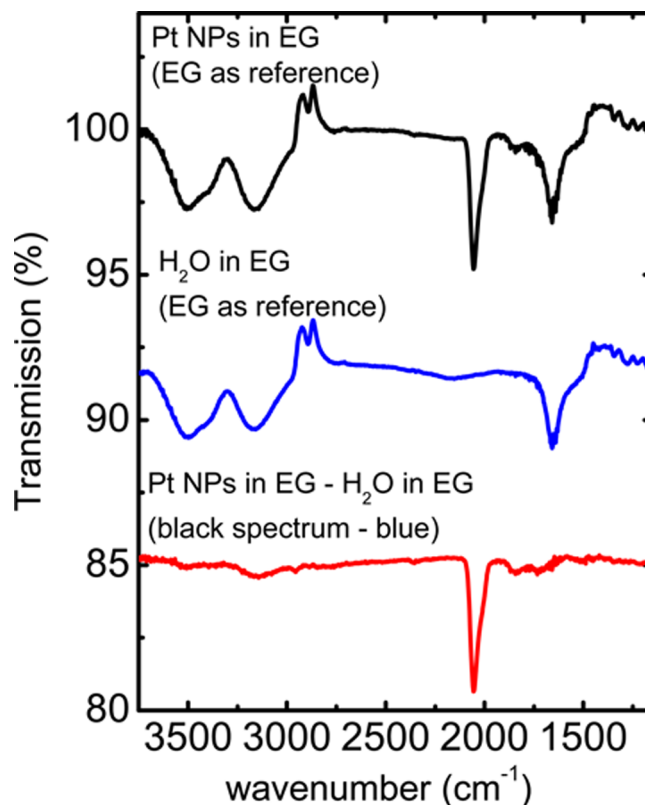


Figure 2. IR spectra of “unprotected” Pt nanoparticles redispersed in EG (black) and H_2O in EG (blue). In both cases pure EG was applied as reference. The blue spectrum was subtracted from the black one in order to account for H_2O residues in the redispersed colloids, which led to the red spectrum.

used to record the spectrum of the “unprotected” nanoparticles was pure EG, as the particles were redispersed in EG for IR spectroscopic characterization. Due to the applied cleaning procedure (section 2.2) any dispersion of redispersed “unprotected” particles usually contains unreproducible amounts of water residues. A pure EG spectrum does thus not correctly represent the required reference for the colloids. For comparison a spectrum of H_2O in EG was recorded (blue spectrum in Figure 2), which demonstrates that most vibrational bands in the “unprotected” Pt colloid spectrum (black spectrum in Figure 2) are related to H_2O residues. The blue spectrum was hence scaled and shifted to achieve a better illustration (see Figure 2) in order to account for the water residues in the particle dispersion and was then subtracted from the blue spectrum of the EG redispersed Pt nanoparticles.

The resulting spectrum of the “unprotected” Pt nanoparticles (red spectrum in Figure 2, transmission values were shifted to achieve a better illustration) clearly reveals a very pronounced signal above 2000 cm^{-1} , which is characteristic for linearly adsorbed CO on Pt. This finding is consistent with the fact that Pt is suitable to oxidize alcohols to form $\text{CO}^{25,26}$ (see reaction pathway 3 shown in Scheme 1).¹⁹ We conclude that “unprotected” Pt nanoparticles are mainly covered by adsorbed CO. In addition two weak bands can be identified at around 1730 and 1830 cm^{-1} . The latter band can be assigned to bridge-bound CO as previously reported for these particles.²⁷ The weak band at 1730 cm^{-1} is characteristic for $\text{C}=\text{O}$ vibrations of carboxyl groups.²⁸ We hence relate this band to glycolate residues in the solvent that were not removed completely by

particle rinsing (see ESI-MS and ^1H NMR spectroscopy results and discussion above). The spectral range above 3000 cm^{-1} that is indicative for O–H vibrations seems to reflect the features of H_2O in EG (blue spectrum). These bands may hence be related to small deviations in the water content of the sample and the background.

The position of the linearly absorbed CO band depends on its vicinity. In a full monolayer or larger CO domains the adsorbed CO is adjacent to other adsorbed CO molecules that vibrate at the same frequency. This causes their dipoles to couple with each other which alters the position of the CO stretching mode. For CO linearly adsorbed on Pt(111) this effect causes a blue-shift of the CO absorption band by around 35 cm^{-1} .²⁹ If adsorbed CO molecules within larger CO domains are replaced by a competing adsorbate, the number of adjacent CO molecules decreases. As a consequence, dipole–dipole coupling diminishes, and the CO stretching mode shifts to lower wavenumbers, until all adjacent CO molecules are replaced. The absorption frequency of such an isolated CO is related to as the singleton frequency.²⁹ The reduction of dipole–dipole coupling is however not the only effect a coadsorbate can have on the position of the CO band. The presence of coadsorbates can also alter the electronic properties of Pt which can in turn affect the π -back-donation strength of the metal to CO. Depending on whether the coadsorbate donates or withdraws electron density it will enhance or reduce the π -back-donation strength, respectively, and consequently induce a shift.

Previously, the position of the CO band of a full CO monolayer on “unprotected” Pt nanoparticles, prepared by the discussed recipe and supported on Al_2O_3 (an inert support that does not alter the electronic structure of the particles), was determined to be around 2060 cm^{-1} .²⁷ For as-prepared “unprotected” Pt nanoparticles, synthesized as described in section 2.1.1, the position of the CO absorption band appears at 2026 cm^{-1} . As this value deviates significantly from the value of a full CO monolayer, we conclude that after synthesis the Pt nanoparticle surface is not covered exclusively by CO. Instead, CO must be partially diluted by another surface species that contributes to the stabilization of the particles. As NMR spectroscopy did not evidence the presence of C–H containing surface-bound species, the only remaining candidate of all proposed stabilizing species is OH^- , which has been previously discussed as the protecting species for Pt nanoparticles prepared via laser ablation in pure H_2O .³⁰ The presence of OH^- on “unprotected” Pt particles can however neither be identified nor excluded on the basis of NMR or IR spectroscopy, as the materials always exhibit residual traces of H_2O .

If the conclusion is correct that “unprotected” Pt nanoparticles prepared by thermal reduction in EG are protected by CO and OH^- , the stability of the resulting colloids should depend critically on the presence of OH^- . In this context it is important to consider that the initial OH^- concentration is not the same as the final OH^- concentration because during the reduction of the metal precursor protons are formed (see Scheme 1). We tested various NaOH starting concentrations (NaOH concentration of the precursor solution before synthesis, see section 2.1.1) and determined that for a concentration of 0.01 M H_2PtCl_6 precursor stable colloids can only be formed with NaOH starting concentrations that are within a range of $0.5\text{--}0.0625\text{ M}$. At higher OH^- concentrations no particle formation occurs, whereas at OH^- starting

concentrations below 0.0625 M particles are formed, which are however not stable under the applied synthesis conditions ($T = 150\text{ }^\circ\text{C}$) but form a black precipitate after several minutes. As the pH scale works only for aqueous media but not for EG, pH measurements are not valid to probe the OH^- concentration before or after synthesis. Nevertheless the final OH^- concentration can be estimated by taking into account that for every generated electron a proton must be formed (see Scheme 1). Using this assumption the final OH^- to $\text{Pt}_{\text{surface atom}}$ ratio was calculated. Thereby, a dispersion (fraction of surface to total number of atoms within the particle) of 96% was taken into account, as previously estimated for Pt nanoparticles prepared by the same recipe.¹⁵ From the resulting dependence (see Figure S5) it is estimated that for a starting OH^- concentration of 0.0615 M NaOH all OH^- is finally neutralized after the reaction. This value is close to the lowest OH^- starting concentration that we determined experimentally for the formation of a stable colloidal dispersion (0.0625 M) evidencing the importance of OH^- to obtain stable colloids that are stable in EG at $150\text{ }^\circ\text{C}$. For the “unprotected” Ru nanoparticles the minimum OH^- concentration to obtain a stable colloidal dispersion is expected to be lower because the Ru (RuCl_3) precursor does not contain protons as compared to the Pt precursor (H_2PtCl_6) and requires only three electrons for complete reduction. Taking this into account a starting OH^- concentration of 0.0308 M was determined, at which all OH^- is neutralized by protons formed within the reaction. Our synthesis tests reveal that down to a OH^- starting concentration of 0.03125 M a stable colloidal dispersion of “unprotected” Ru can be prepared with RuCl_3 . These calculations hence support the hypothesis that not merely CO but also OH^- is needed to form a stable colloidal dispersion under the applied synthesis conditions.

If “unprotected” nanoparticles are indeed protected by CO and OH^- , the coverage of the two has to depend on the CO/ OH^- ratio. It is expected that the OH^- coverage increases as the initial NaOH concentration is increased. Concurrently, the CO coverage has to decrease. In order to test for this hypothesis, the CO stretching mode of as-prepared “unprotected” Pt colloids prepared with various NaOH concentrations was probed by IR spectroscopy. The position of the CO band with respect to the initial OH^- concentration and the final $\text{OH}^-/\text{Pt}_{\text{surface atom}}$ ratio, determined from Figure S5, are shown in Table 1.

The position of the CO band shifts from 2020 cm^{-1} for the highest OH^- starting concentration (0.5 M) to higher wavenumbers, as the OH^- concentration is decreased. OH^-

Table 1. Starting NaOH Concentration and the Corresponding Ratio of OH^- to $\text{Pt}_{\text{surface atom}}$ after Synthesis Are Shown^a

starting NaOH concentration (M)	final ratio of $\text{OH}^-/\text{Pt}_{\text{surface atoms}}$	CO band position (cm^{-1})
0.5	44.5	2020
0.25	19.1	2026
0.125	6.4	2031
0.09375	3.3	2037
0.078125	1.7	2042
0.0625	0.1	2046

^aFurthermore the positions of the CO stretching mode with respect to the OH^- concentration are listed.

is an electron-donating adsorbate. It may hence increase the electron density of Pt and in turn enhance the strength of π -back-donation from Pt to CO. Also, adsorbed OH^- may dilute the surface CO thus reducing dipole–dipole coupling. Irrespective of which effect is the more dominant, both may cause the same trend for the CO band to shift to lower wavenumbers for increasing OH^- concentrations. The position of the CO band of the colloids prepared with the lowest OH^- concentration appears at 2046 cm^{-1} , which is still about 14 cm^{-1} below the value for a full CO monolayer on these particles (2060 cm^{-1}).²⁷ This finding indicates that for “unprotected” Pt nanoparticles prepared with the lowest suitable OH^- concentration the particles are still not fully covered by CO nor do they exhibit larger domains of adjacent CO. It thus seems likely that for obtaining stable colloids under the applied synthesis conditions the particles have to be covered by OH^- and CO. The signal-to-noise ratio for as-prepared Ru nanoparticles was unfortunately too low to allow for a meaningful determination of the CO band position. An explanation is given in the SI.

Finally, the influence of the OH^- concentration on the resulting particle size distribution was investigated by small-angle X-ray scattering (SAXS). Three representative distributions are shown in Figure 3, with the OH^- concentration decreasing in the following order: black > red > blue.

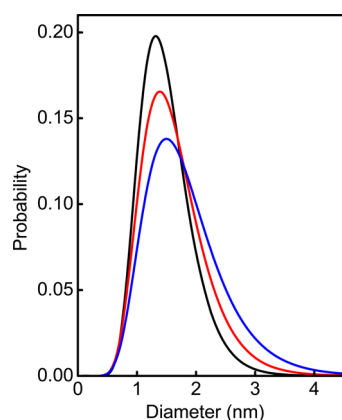


Figure 3. Particle size distributions determined from SAXS measurements for “unprotected” Pt nanoparticles prepared with a starting NaOH concentration of 0.25 M NaOH (black), 0.09375 M NaOH (red), and 0.078125 M NaOH (blue). As the OH^- concentration is lowered, the maximum shifts to larger particle diameters, and the distributions broaden.

The different size distributions reveal that the maximum is shifted to larger diameters, when the OH^- concentration is decreased, and that the size distributions broaden. This finding can be explained by the conclusion that the second protecting species is OH^- . As the OH^- concentration is lowered the availability of OH^- for the protection of the particles under synthesis conditions decreases. This means that smaller particles are less effectively protected, and the probability that they grow increases. When all OH^- is neutralized by protons formed within the reaction (see Scheme 1) no OH^- is left for the stabilization of the particles. As a consequence, the particles are no longer stabilized and start to agglomerate to form a black precipitate.

Our findings demonstrate that varying the NaOH concentration for the synthesis of nanoparticles in EG enables only for

a very limited control over the particle size. In order to further tune the particle size, one has to work without NaOH. This however requires the use of a different protecting agent. The most common strategy is to add poly(vinylpyrrolidone) (PVP) to EG which enables controlling the size of Pt nanoparticles in a range of 1–7 nm.³¹ This however means that the colloids are no longer related to as “unprotected” because PVP-protected particles require a thermal or ozone treatment in order to unveil their entire catalytic surface.³² In the original recipe for “unprotected” Pt nanoparticles it has been proposed that the size of “unprotected” Pt nanoparticles can be tuned up to 4 nm by adding H_2O to the reaction medium.⁸ The applicability of this approach is however limited by the fact that adding H_2O leads to a substantial loss of the expensive metal as most of the particles precipitate. Tuning the size of “unprotected” nanoparticles over a broader range than that shown in Figure 3 hence remains a challenging task, and new synthetic ideas will be needed in order to overcome this limitation.

4. CONCLUSION

Nanoparticles that are related to as “unprotected” because they are prepared in alkaline EG without use of any strongly binding stabilizing agent were characterized by NMR and IR spectroscopy. No evidence for the presence of C–H containing species was found. Instead, IR spectroscopy revealed the particles to be covered by CO and a second adsorbate with the latter not being identifiable spectroscopically. On the basis of the spectroscopic characterization and synthetic tests with different NaOH concentrations the coadsorbate is postulated to be OH^- . It was shown that for the applied synthesis conditions ($T = 150\text{ }^\circ\text{C}$ in EG) the presence of OH^- is essential in order to obtain stable colloids. The influence of the OH^- concentration on the particle size distribution was probed by SAXS, and the results evidence that the particle size increases and the distribution broadens as the OH^- concentration is lowered. Variation of the OH^- concentration however enables only for limited change in particle size. Our next aim is hence to search for new synthetic ideas in order to achieve a better control over the particle size for “unprotected” nanoparticles than reported here.

■ ASSOCIATED CONTENT

Supporting Information

The Supporting Information is available free of charge on the ACS Publications website at DOI: 10.1021/acs.jpcc.5b03863. ESI-MS spectra of supernatant after particle precipitation, NMR spectra of “unprotected” Pt NPs after adding EG and glycolic acid, NMR spectrum of “unprotected” Ru NPs, graph illustrating the dependence of the final OH^- to surface atom ratio with respect to the initial NaOH concentration for Pt and Ru NPs, and representative IR spectrum dried “unprotected” Ru NPs (PDF)

■ AUTHOR INFORMATION

Corresponding Author

*Tel.: +49-421-218 63187. E-mail: sebkunz@uni-bremen.de.

Notes

The authors declare no competing financial interest.

■ ACKNOWLEDGMENTS

I. S. and S. K. gratefully acknowledge the “Fonds der Chemischen Industrie” (FCI) for financial support. M.A.

acknowledges support from Danish Council for Strategic Research (4M Center).

REFERENCES

- (1) Xia, Y. N.; Xiong, Y. J.; Lim, B.; Skrabalak, S. E. Shape-Controlled Synthesis of Metal Nanocrystals: Simple Chemistry Meets Complex Physics? *Angew. Chem., Int. Ed.* **2009**, *48*, 60–103.
- (2) Park, J.; Joo, J.; Kwon, S. G.; Jang, Y.; Hyeon, T. Synthesis of Monodisperse Spherical Nanocrystals. *Angew. Chem., Int. Ed.* **2007**, *46*, 4630–4660.
- (3) Toshima, N.; Yonezawa, T. Bimetallic Nanoparticles - Novel Materials for Chemical and Physical Applications. *New J. Chem.* **1998**, *22*, 1179–1201.
- (4) Zhang, Y. W.; Grass, M. E.; Kuhn, J. N.; Tao, F.; Habas, S. E.; Huang, W. Y.; Yang, P. D.; Somorjai, G. A. Highly Selective Synthesis of Catalytically Active Monodisperse Rhodium Nanocubes. *J. Am. Chem. Soc.* **2008**, *130*, 5868–5869.
- (5) Huang, W. X.; Hua, Q.; Cao, T. Influence and Removal of Capping Ligands on Catalytic Colloidal Nanoparticles. *Catal. Lett.* **2014**, *144*, 1355–1369.
- (6) Kunz, S.; Iglesia, E. Mechanistic Evidence for Sequential Displacement–Reduction Routes in the Synthesis of Pd–Au Clusters with Uniform Size and Clean Surfaces. *J. Phys. Chem. C* **2014**, *118*, 7468–7479.
- (7) Fievet, F.; Lagier, J. P.; Blin, B.; Beaudoin, B.; Figlarz, M. Homogeneous and Heterogeneous Nucleations in the Polyol Process for the Preparation of Micron and Submicron Size Metal Particles. *Solid State Ionics* **1989**, *32–33*, 198–205.
- (8) Wang, Y.; Ren, J. W.; Deng, K.; Gui, L. L.; Tang, Y. Q. Preparation of Tractable Platinum, Rhodium, and Ruthenium Nanoclusters with Small Particle Size in Organic Media. *Chem. Mater.* **2000**, *12*, 1622–1627.
- (9) Wang, X. D.; Stover, J.; Zielasek, V.; Altmann, L.; Thiel, K.; Al-Shamery, K.; Baumer, M.; Borchert, H.; Parisi, J.; Kolny-Olesiak, J. Colloidal Synthesis and Structural Control of Pt₂ Bimetallic Nanoparticles. *Langmuir* **2011**, *27*, 11052–11061.
- (10) Fu, X. Y.; Wang, Y.; Wu, N. Z.; Gui, L. L.; Tang, Y. Q. Surface Modification of Small Platinum Nanoclusters with Alkylamine and Alkylthiol: An Xps Study on the Influence of Organic Ligands on the Pt 4f Binding Energies of Small Platinum Nanoclusters. *J. Colloid Interface Sci.* **2001**, *243*, 326–330.
- (11) Wang, X.; Sonstrom, P.; Arndt, D.; Stover, J.; Zielasek, V.; Borchert, H.; Thiel, K.; Al-Shamery, K.; Baumer, M. Heterogeneous Catalysis with Supported Platinum Colloids: A Systematic Study of the Interplay between Support and Functional Ligands. *J. Catal.* **2011**, *278*, 143–152.
- (12) Speder, J.; Altmann, L.; Roefzaad, M.; Baeumer, M.; Kirkensgaard, J. J. K.; Mortensen, K.; Arenz, M. Pt Based Pemfc Catalysts Prepared from Colloidal Particle Suspensions - a Toolbox for Model Studies. *Phys. Chem. Chem. Phys.* **2013**, *15*, 3602–3608.
- (13) Speder, J.; Altmann, L.; Bäumer, M.; Kirkensgaard, J. J.; Mortensen, K.; Arenz, M. The Particle Proximity Effect: From Model to High Surface Area Fuel Cell Catalysts. *RSC Adv.* **2014**, *4*, 14971–14978.
- (14) Speder, J.; Zana, A.; Spanos, I.; Kirkensgaard, J. J. K.; Mortensen, K.; Hanzlik, M.; Arenz, M. Comparative Degradation Study of Carbon Supported Proton Exchange Membrane Fuel Cell Electrocatalysts – the Influence of the Platinum to Carbon Ratio on the Degradation Rate. *J. Power Sources* **2014**, *261*, 14–22.
- (15) Kunz, S.; Schreiber, P.; Ludwig, M.; Maturi, M. M.; Ackermann, O.; Tschurl, M.; Heiz, U. Rational Design, Characterization and Catalytic Application of Metal Clusters Functionalized with Hydrophilic, Chiral Ligands: A Proof of Principle Study. *Phys. Chem. Chem. Phys.* **2013**, *15*, 19253–19261.
- (16) Morsbach, E.; Spéder, J.; Arenz, M.; Brauns, E.; Lang, W.; Kunz, S.; Bäumer, M. Stabilizing Catalytically Active Nanoparticles by Ligand Linking: Toward Three-Dimensional Networks with High Catalytic Surface Area. *Langmuir* **2014**, *30*, 5564–5573.
- (17) Ertl, G.; Küppers, J. *Low Energy Electrons and Surface Chemistry*; Verlag Chemie: 1983.
- (18) Yang, J.; Deivaraj, T. C.; Too, H. P.; Lee, J. Y. Acetate Stabilization of Metal Nanoparticles and Its Role in the Preparation of Metal Nanoparticles in Ethylene Glycol. *Langmuir* **2004**, *20*, 4241–4245.
- (19) Bock, C.; Paquet, C.; Couillard, M.; Botton, G. A.; MacDougall, B. R. Size-Selected Synthesis of Pt₂ Nano-Catalysts: Reaction and Size Control Mechanism. *J. Am. Chem. Soc.* **2004**, *126*, 8028–8037.
- (20) Schrader, I.; Warneke, J.; Backenköhler, J.; Kunz, S. Functionalization of Platinum Nanoparticles with L-Proline: Simultaneous Enhancements of Catalytic Activity and Selectivity. *J. Am. Chem. Soc.* **2015**, *137*, 905–912.
- (21) Hens, Z.; Martins, J. C. A Solution Nmr Toolbox for Characterizing the Surface Chemistry of Colloidal Nanocrystals. *Chem. Mater.* **2013**, *25*, 1211–1221.
- (22) Wu, Z.; Gayathri, C.; Gil, R. R.; Jin, R. Probing the Structure and Charge State of Glutathione-Capped Au-25(Sg)(18) Clusters by Nmr and Mass Spectrometry. *J. Am. Chem. Soc.* **2009**, *131*, 6535–6542.
- (23) Tong; Rice, C.; Godbout, N.; Wieckowski, A.; Oldfield, E. Correlation between the Knight Shift of Chemisorbed Co and the Fermi Level Local Density of States at Clean Platinum Catalyst Surfaces. *J. Am. Chem. Soc.* **1999**, *121*, 2996–3003.
- (24) van der Klink, J. J.; Brom, H. B. Nmr in Metals, Metal Particles and Metal Cluster Compounds. *Prog. Nucl. Magn. Reson. Spectrosc.* **2000**, *36*, 89–201.
- (25) Sexton, B. A.; Rendulic, K. D.; Huges, A. E. Decomposition Pathways of C1-C4 Alcohols Adsorbed on Platinum (111). *Surf. Sci.* **1982**, *121*, 181–198.
- (26) Lee, A. F.; Gawthrop, D. E.; Hart, N. J.; Wilson, K. A Fast Xps Study of the Surface Chemistry of Ethanol over Pt {111}. *Surf. Sci.* **2004**, *548*, 200–208.
- (27) Altmann, L.; Kunz, S.; Bäumer, M. Influence of Organic Amino and Thiol Ligands on the Geometric and Electronic Surface Properties of Colloidally Prepared Platinum Nanoparticles. *J. Phys. Chem. C* **2014**, *118*, 8925–8932.
- (28) Günzler, H.; Gremlich, H. U. *IR Spectroscopy: An Introduction*; Wiley: New York, 2002.
- (29) Hoffmann, F. M. Infrared Reflection-Absorption Spectroscopy of Adsorbed Molecules. *Surf. Sci. Rep.* **1983**, *3*, 107–192.
- (30) Marzun, G.; Streich, C.; Jendrzey, S.; Barcikowski, S.; Wagener, P. Adsorption of Colloidal Platinum Nanoparticles to Supports: Charge Transfer and Effects of Electrostatic and Steric Interactions. *Langmuir* **2014**, *30*, 11928–11936.
- (31) Song, H.; Rioux, R. M.; Hoefelmeyer, J. D.; Komor, R.; Niesz, K.; Grass, M.; Yang, P. D.; Somorjai, G. A. Hydrothermal Growth of Mesoporous Sba-15 Silica in the Presence of Pvp-Stabilized Pt Nanoparticles: Synthesis, Characterization, and Catalytic Properties. *J. Am. Chem. Soc.* **2006**, *128*, 3027–3037.
- (32) Park, J. Y.; Aliaga, C.; Renzas, J. R.; Lee, H.; Somorjai, G. A. The Role of Organic Capping Layers of Platinum Nanoparticles in Catalytic Activity of Co Oxidation. *Catal. Lett.* **2009**, *129*, 1–6.